Title: Multisite phosphorylation regulates phenotypic variability in antibiotic tolerance

Authors: Elizabeth A. Libby [1,2,3], Shlomi Reuveni [2,4,5,6], and Jonathan Dworkin [*,1]

Affiliations:

[1]Department of Microbiology & Immunology, College of Physicians and Surgeons, Columbia University, New York, NY 10032 USA

[2]Department of Systems Biology, Harvard Medical School, Boston, MA 02115

[3]Wyss Institute for Biologically Inspired Engineering, Harvard University, Boston, MA 02115

[4]School of Chemistry, Tel-Aviv University, Tel-Aviv 6997801, Israel

[5]Center for the Physics and Chemistry of Living Systems. Tel Aviv University, 6997801, Tel Aviv, Israel.

[6]The Sackler Center for Computational Molecular and Materials Science, Tel Aviv University, 6997801, Tel Aviv, Israel.

*Corresponding author, jonathan.dworkin@columbia.edu, 212.342.3731 (tel)

Classification: Biological Sciences, Microbiology

Keywords: antibiotic tolerance, noise, (p)ppGpp, phenotypic variability, Ser/Thr kinase, kinase inhibitors, Gram-positive bacteria, eSTK, eSTP, two-component systems.

Abstract:

Isogenic populations of cells exhibit phenotypic variability that has specific physiological consequences. For example, individual bacteria can differ in their sensitivity to an antibiotic, but whether this variability is regulated or an unavoidable consequence of stochastic fluctuations is unclear. We observed that a bacterial stress response gene, the (p)ppGpp synthetase *sasA*, exhibits high levels of extrinsic noise in expression, suggestive of a regulatory process. We traced this variability to the convergence of two signaling systems that together control an event largely unexplored in bacteria, the multisite phosphorylation of a transcription factor. We found that this regulatory intersection is crucial for controlling the appearance of outliers, rare cells with unusually high levels of *sasA* expression. Additionally, by examining the full distributions of gene expression we calculated the importance of multisite phosphorylation in setting the relative abundance of cells with a given a level of SasA. We then created a predictive model for the probability of a given cell surviving antibiotic treatment as a function of *sasA* expression. Therefore, our data show that multisite phosphorylation can be used to strongly regulate bacterial physiology and sensitivity to antibiotic treatment.

Significance Statement:

Cells possess many signaling pathways for sensing and responding to their environment. Although these pathways are commonly characterized individually, signals between separate pathways are often integrated. One way that pathways can intersect is through multisite phosphorylation controlling the activity of a common target, where each phosphorylation is contributed by a separate signaling system. Bacteria are an ideal place to study the effects of these intersections on gene expression since the number of such intersections is comparatively small, and subsequent gene regulation relatively simple. Here we show that signal integration through multisite phosphorylation is important for setting the frequency of bacterial cells with

44 increased antibiotic tolerance by controlling the heterogeneity, or noise, in gene expression

45 across the population.

46

\body

Introduction:

Many bacterial phenotypes, including antibiotic tolerance and virulence, often reflect the phenotype of a subset of the population rather than the average behavior (1, 2). Subpopulations of bacteria can arise through purely stochastic processes as well as by regulatory and signaling pathways (3). Theoretically, one way to create phenotypic diversity via a signaling pathway is multisite phosphorylation (4, 5). However, it has not been experimentally shown that multisite phosphorylation regulates variation in gene expression between cells, and subsequently, the emergence of phenotypic diversity in bacterial populations. Recently, multisite phosphorylation of transcription factors have been observed in pathways involved in antibiotic tolerance and virulence (6), suggesting that dynamics of multisite phosphorylation could have particular physiological relevance.

Bacterial signaling is often conceptualized in the context of two-component signal transduction systems (TCS) that generally consist of a histidine kinase that phosphorylates a response regulator on a single residue, which then acts as a transcription factor (7). The stimulus-dependent response of this type of signaling system architecture has been analyzed theoretically (8, 9) and experimentally (10, 11), with little cell-to-cell variability observed, regardless of inducer level. This suggests that extensive cell-to-cell variability is not a general feature of bacterial TCS. However, some notable exceptions have been found for two-component systems with more complex architectures, such as the broad distribution of gene expression in the TorS/TorR regulon in *E. coli* (12) which has recently been shown to be an important factor for cell survival during oxygen depletion (13). The network architecture of bacterial signal transduction systems may therefore play an as yet underappreciated role in the dynamics and survival of bacterial populations.

It has been apparent for over 60 years that bacterial populations contain rare cells that display increased phenotypic resistance to antibiotics (14). These cells, presumed to be quiescent, have been implicated in antibiotic treatment failure in genetically susceptible bacterial infections (15). To date, it remains unclear to what extent the appearance of these rare cells, is subject to regulation. Emerging evidence strongly implicates elevated levels of the nucleotide second messenger (p)ppGpp as a causative agent of quiescence in many bacterial species (16-19). (p)ppGpp downregulates essential cellular processes such as transcription, translation, and DNA replication (20). Although the precise mechanism of (p)ppGpp synthesis and its direct cellular targets vary between bacterial species, highly elevated levels of (p)ppGpp confer a quiescent state to the bacterial cell. As many antibiotics target active cellular processes, the resulting cells exhibit increased antibiotic tolerance, suggesting that cell-to-cell variability in (p)ppGpp may be involved in phenotypic resistance to antibiotics (19, 21-23).

The mechanistic origin of cell-to-cell variability in (p)ppGpp levels across bacterial populations remains a major open question. To date, this has been best studied in *E. coli*, which has two bi-functional (p)ppGpp synthetase-hydrolases (RelA and SpoT) (24). In contrast, other bacterial species often possess dedicated (p)ppGpp synthetases, termed small alarmone synthtases (SAS), in addition to bi-functional synthetase-hydrolases (25). These SAS proteins can be activated transcriptionally (20), suggesting that cell-to-cell variability in (p)ppGpp levels could originate in the transcriptional regulation of the synthetases themselves. In the Gram-positive bacterium *B. subtilis*, (p)ppGpp synthesis is regulated by three distinct proteins: RelA, SasA, and SasB (26). *B. subtilis* RelA is a bi-functional (p)ppGpp synthetase-hydrolase, and both SasA and SasB are dedicated synthetases. Although *relA* and *sasB* transcripts are both readily detectable during log phase growth, *sasA* (formerly *ywaC*) transcripts are found at considerably lower levels. However, *sasA* is inducible by certain classes of cell-wall-active antibiotics (27, 28), and its induction by alkaline shock increases the cellular levels of ppGpp (26). Since *sasA* expression

stops growth (29), SasA-mediated (p)ppGpp synthesis provides a mechanism to induce cellular quiescence in response to environmental stresses. To date, SasA is only known to be regulated transcriptionally, so significant cell-to-cell variability in *sasA* expression could produce physiologically relevant cell-to-cell variability in (p)ppGpp levels.

In this work, we demonstrate that *sasA* expression displays physiologically relevant amounts of extrinsic noise, although the average level of *sasA* expression is very low during growth. Furthermore, we find that the distribution of *sasA* expression and the frequency of outliers are strongly regulated by the activity of a highly conserved eukaryotic-like Ser/Thr kinase system and its subsequent multisite phosphorylation of a transcription factor. Using quantitative analysis of the full distributions of *sasA* expression, we find that multisite phosphorylation is responsible for exponentially regulating the abundance of cells with a given level of SasA and generate a predictive model for *sasA*-expression-dependent antibiotic tolerance.

Results:

While the population average level of *sasA* expression during growth is extremely low (27), the average behavior may mask important phenotypic variation between cells. We therefore generated a transcriptional reporter for *sasA* (P_{sasA}-*yfp*) to study the population at the single-cell level. Surprisingly, there was considerable cell-to-cell variability in P_{sasA}-*yfp* (coefficient of variation, CV~4.95 ± 0.42, mean ± SEM), with most cells having very low expression, and rare cells showing significantly higher levels of expression (Fig. 1A). Quantification of YFP fluorescence revealed that a small fraction of the population had much higher (>~10x) levels of fluorescence than the mean, and rare cells had ~100x.

The high levels of cell-to-cell variability in *sasA* expression could be caused by intrinsic noise from the promoter itself, or by extrinsic noise originating in an upstream process (32). To differentiate between these mechanisms, we used a strain with dual fluorescent reporters, P_{sasA}-*yfp* and P_{sasA}-*mcherry* (Fig. 1B). Expression of the dual reporters in individual cells was highly

122 correlated (Pearson's correlation coefficient, r~0.90±0.08, mean ± SEM), demonstrating that the
123 noise was largely extrinsic to the promoter (Fig. 1C, D).

124 To determine if variation in YFP levels were simply caused by global changes in the population
125 that result in the accumulation of large amounts of fluorescent protein (33), P_{sasA}-*yfp* was
126 compared to a presumably unrelated promoter known to be constitutive during log phase growth,
127 P_{veg}-*mcherry* (34) (Fig. S1). We found that YFP and mCherry levels were not highly correlated,
128 suggesting that the high levels of variability in *sasA* expression are caused by a *sasA*-specific
129 pathway. We then tested a previously characterized *sasA* regulator, the sigma factor σ^M (SigM)
130 (35), that is required for *sasA* expression (28) (Fig. S2A, B). However, *sasA* expression also did
131 not correlate strongly with *sigM* expression (Fig. S2C, D).

132 Another potential regulator of *sasA* is the WalR transcription factor observed to bind the *sasA*
133 promoter in a genome-wide screen (36). WalR is the response regulator of the essential WalRK
134 two-component system and is activated by phosphorylation of Asp-53 by WalK (37). Once
135 phosphorylated, WalR can either activate or repress genes in its regulon. A reversible second
136 phosphorylation on WalR Thr-101 by the eukaryotic-like Ser/Thr kinase-phosphatase pair
137 PrkC/PrpC (30) further potentiates WalR activity at both activating and repressing sites (31). In
138 rich media (LB), the multisite phosphorylation of WalR affects gene expression (*e.g.*, enhanced
139 activation of *yocH*) specifically in post-log phase (31). However, in commonly used defined
140 minimal media (S7-glucose), there is a consistent PrkC-dependent effect on the population
141 average level of *yocH* expression throughout log phase (Fig. S3). As *sasA* is known to be
142 activated by antibiotics such as bacitracin (27), we first tested whether the PrkC/PrpC – WalR
143 system regulates *sasA* at the population level to determine if WalR activates or represses *sasA*.
144 We found that PrkC activity represses *sasA* expression through WalR Thr101~P during bacitracin
145 treatment (Fig. S4). Based on these bulk measurements, we developed a model for *sasA*
146 regulation (Fig. 2A) in which PrkC activity further potentiates WalR-repressing activity at *sasA*

147 through a second phosphorylation of WalR at Thr-101. However, it remained unclear to what
148 extent multisite phosphorylation of WalR affects cell-to-cell variability in *sasA* expression.

149 Cell-to-cell variability in gene expression can be tuned by changing repressor-binding affinities
150 (38, 39), suggesting that multisite phosphorylation of WalR may play a critical role in setting the
151 observed distribution of *sasA* expression across the population. To test this, we measured the
152 distribution of *sasA* expression in wild type (WT) cells and compared it to genetic backgrounds
153 that alter the phosphorylation state of WalR: Δ*prpC* (no phosphatase, high levels of T101~P), and
154 Δ*prkC* (no kinase, no detectable T101~P) (Fig. 2B). Qualitatively, in the Δ*prpC* background, the
155 frequency of cells with high levels of *sasA* expression was strongly reduced, whereas it was
156 strongly increased in the Δ*prkC* background. The PrpC-dependent effect on *sasA* expression
157 requires PrkC, since the distribution of *sasA* expression in a strain lacking both the kinase and
158 phosphatase (Δ(*prpC-prkC*)) is very similar to a strain lacking just the kinase.

159 We first sought to quantify the effect of WalR multisite phosphorylation on the frequency of
160 "outliers": cells with a level of *sasA* expression above a fixed threshold in each population. We
161 therefore compared independent measurements of the distribution of *sasA* expression in WT,
162 Δ*prpC*, and Δ(*prpC-prkC*) backgrounds (Fig. 2C, left) and found that PrkC significantly affects the
163 mean frequency of outliers >8 fold by this measure (*walR* ^{WT}, Δ*prpC* vs Δ(*prpC-prkC*): **p-
164 value~0.004, Kolmogorov-Smirnov test). We repeated the measurements in a *walR* ^{T101A}
165 background (Fig. 2C, right) and found that PrkC no longer has a significant effect on the mean
166 frequency of outliers in the phosphosite mutant background (*walR* ^{T101A}, Δ*prpC* vs Δ(*prpC-prkC*):
167 p-value~0.56, ns, Kolmogorov-Smirnov test). These results are consistent with increased WalR
168 activity by Thr-101 phosphorylation causing increased repression of *sasA*, and thereby regulating
169 the frequency of *sasA* outliers (Fig. 2D).

Analyzing the absolute frequency of outliers, however, relies on the definition of a cutoff threshold and therefore does not fully address how multisite phosphorylation affects the entire distribution of *sasA* expression across the population. To quantify the effect of PrkC on the distribution of cell-to-cell variability in *sasA* expression, we deconvolved the measured data from the cellular autofluorescence (SI). This resulted in autofluorescence-free distributions of *sasA* expression, allowing better quantitative comparison of expression between genetic backgrounds (Fig. 3A). This deconvolution method uses only the first two moments (i.e., the mean and variance) of the observed distributions of fluorescence. As such, the auto-fluorescence free distributions are relatively insensitive to the observed "outliers" in each distribution, but makes a statistical prediction for those frequencies. To verify the accuracy of the predictions, these calculated distributions were re-convolved with the cellular autofluorescence and the reconstructed data set compared to the original data (Fig. S5). Calculation of the relative enrichment of cells with a given level of *sasA* in each genetic background revealed that maximal T101~P (Δ*prpC*) compared to no T101~P (Δ*prkC*) results in exponential changes in the relative abundance of cells at a given level of *sasA* (Fig. 3B).

Together, the model and the outlier analysis in Fig. 2 suggest that PrkC-dependent regulation of the distribution of *sasA* expression requires the second phosphosite at WalR T101. To test this, we repeated the deconvolution procedure for a strain expressing a WalR mutant that lacks the Thr-101 phosphosite, *walR T101A*, and found that the PrkC-dependent effect on *sasA* expression is indeed WalR Thr-101-dependent (Fig. 3C, Fig. S6A). Thus, multisite phosphorylation is responsible for the exponential depletion of cells with medium to high levels of *sasA* expression in the Δ*prpC* background (Fig. 3B).

We then measured how intermediate levels of multisite phosphorylation regulate the distribution of *sasA* expression using the kinase inhibitor staurosporine to progressively inhibit PrkC activity (40) (Figs. S6B; S7). The distributions of *sasA* expression were again deconvolved

(Fig. S6C), and we calculated the relative enrichment of cells with a given level of *sasA* fluorescence at increasing concentrations of staurosporine (Fig. 3D). Titration of PrkC activity resulted in exponential enrichment of cells with a given level of *sasA*. Therefore, even small changes in PrkC activity result in large changes in the abundance of "outliers", cells with unusually high levels of *sasA*.

Since SasA is a (p)ppGpp synthetase, we sought to determine the approximate level of *sasA* expression at which increased amounts of (p)ppGpp affect cell physiology. To do so, we used a transcriptional reporter for *ilvA*, a gene that is upregulated in response to an increase in (p)ppGpp levels (41). Although a direct mapping between absolute levels of (p)ppGpp and *ilvA* expression has not been established, we reasoned that cells which exhibit a correlated and *sasA*-dependent increase in *ilvA* expression would have a physiologically relevant level of *sasA* expression. We observed this increase in cells with *sasA* levels above a certain threshold (Fig. 4A), suggesting that even in the absence of induction some cells in WT populations have physiologically relevant levels of *sasA*.

Elevated levels of (p)ppGpp confer a quiescent state to the bacterial cell resulting in antibiotic tolerance (23, 42). Cell-to-cell variability in (p)ppGpp production has been proposed to result in cell-to-cell variability in antibiotic survival (43, 44). However, a direct and quantitative relationship between the expression of a (p)ppGpp synthetase and the probability of survival for an individual cell has not been demonstrated. We therefore sought to determine if cells with pre-existing high levels of *sasA* preferentially survive antibiotic exposure, and if so, provide a model for how the level of *sasA* expression influences the probability of survival for a given cell.

We used ciprofloxacin, a DNA gyrase inhibitor that does not significantly increase the population average level of *sasA* expression (27). We measured (Fig. S8) and deconvolved (Fig. 4B,C) the distributions of *sasA* expression (P_{sasA}-*yfp*) both pre-and post-ciprofloxacin treatment that results in ~99% killing in both WT and Δ*sasA* backgrounds. Using these distributions, we

calculated the relative enrichment of cells with a given level of *sasA* following antibiotic treatment (Fig. 4D), yielding a simple model for the effect of antibiotic treatment on the distribution of *sasA* expression (SI). Because antibiotic treatments can be affected by many processes, we separated out the size of the *sasA*-dependent effect by using a Δ*sasA* mutant as a control. WT populations exhibited a significant increase in the fraction of cells with elevated levels of *sasA* (Fig. 4D). This effect is strongly reduced in the Δ*sasA* background, demonstrating that a substantial part of the enrichment, particularly at high levels of *sasA* expression, is *sasA*-dependent.

We then sought to determine whether our enrichment model reflects the probability of survival for cells as a function of *sasA* expression. Since SasA is a (p)ppGppp synthetase, the *sasA*-dependent enrichment we observe post-ciprofloxacin treatment could be due to an expression-dependent probability of surviving antibiotic treatment. Alternately, since the measured increase in mean fluorescence was relatively small (~2 fold), it is also possible that ciprofloxacin acts in a complex, expression-dependent, manner to generate the observed post-treatment distribution of *sasA* expression but does not affect survival. To differentiate between these hypotheses, we used FACS to sort bacteria prior to ciprofloxacin treatment from both WT and Δ*sasA* populations into "high" (upper ~1%) and "low" (~average) P_{sasA}-*yfp* expression groups (Fig. 4E). Following ciprofloxacin treatment (as in Figs. 4B,C, S8), the relative survival of "high" and "low" expression cells, or the survival ratio, was assayed by plating for CFUs (Fig. 4F). The average fluorescence cutoff values used in the FACS experiments, low: 4.1±1.8 and high: 779.5±134.9 (mean ± SEM, 3 experiments), were then used as inputs for a model where the enrichment of cells with increased levels of *sasA* (Fig. 4D) is caused by increased survival (SI). The model yielded good agreement with the results of the FACS experiments: it predicted relative survival ratios of ~9 for wild-type, and ~2 for Δ*sasA*, respectively, compared to the measured values of ~9.5 ± 0.6 (WT) and 1.8 ± 0.7 (Δ*sasA*) (Fig. 4F). Therefore, the enrichment of cells with elevated levels of *sasA* post-ciprofloxacin treatment can be largely attributed to the increased survival probability of pre-existing cells in the population with elevated *sasA* expression.

Taken together, our results demonstrate that an important consequence of PrkC-dependent multisite phosphorylation of WalR is the regulation of cell-to-cell variability, or noise, in the WalR regulon gene *sasA*. By comparing the full distributions of gene expression, we demonstrate that this effect is not just confined to the regulation of outliers in gene expression above an arbitrary threshold within the population, but has an exponential effect on the relative abundance of cells with a given level of expression. By analyzing the full distributions of expression we are also able to demonstrate that *sasA* expression also continuously affects the antibiotic tolerance of individual cells: specifically, the survival probability during a fixed course antibiotic treatment. This model (SI) is consistent with cell sorting experiments that explicitly demonstrate that the observed distributions are a consequence of survival probability.

Discussion:

Antibiotic tolerance is believed to be an important factor in the failure of antibiotic treatments and a key step toward the development of antibiotic resistance (45). We therefore sought to trace the origin of the cell-to-cell variability in expression of *sasA* and determine if it can be regulated by genetic or chemical means. Noise in gene expression can be conceptually separated into intrinsic and extrinsic noise. Although it is difficult to design strategies to specifically target events generated by intrinsic noise, extrinsic noise may have upstream regulatory pathways that can be modulated. Therefore, it is significant that the cell-to-cell variability in *sasA* was dominated by extrinsic noise at high levels of expression (Fig.1) that have the strongest effect on antibiotic tolerance (Fig. 4). Furthermore, since multisite phosphorylation is responsible for setting the observed distribution of cell-to-cell variability (Figs. 2, 3), this regulatory pathway could be a novel antibiotic target.

Multisite phosphorylation can expand the range of a protein's function, generating both switch-like (46, 47), and graded (48, 49) changes in average activity. In contrast, here we observed only minimal changes in the average levels of *sasA* expression as a function of PrkC activity, but

measured up to a ~100-fold effect on the frequency of "outliers", cells with particularly high levels of expression (Fig. 3B). This response was shown to be graded, rather than switch-like, likely arising as a consequence of the integration of signals from two distinct signaling systems. A single phosphorylation at WalR Asp-53 strongly, but imperfectly, represses the *sasA* promoter. The addition of the second phosphorylation at Thr-101 by a distinct signaling system then acts as a second input to further regulate WalR. Interestingly, even small changes in activity of the second system result in marked changes in the frequency of outliers.

Transcriptional regulation of outliers in eukaryotes has been shown to be predictive of which cancer cells survive drug treatment (50). Here we found that transcriptional regulation by multisite phosphorylation is also critical for setting the pre-existing distribution of survival probabilities for cells within a bacterial population. Distinct from bacterial persistence, which is characterized by bi-phasic killing, these survival probabilities reflect antibiotic tolerance or the killing kinetics during a relatively short, fixed time-course, antibiotic treatment (51). In the Δ*sasA* background, we observed a much weaker dependence of antibiotic tolerance on *sasA* expression. This residual dependence is consistent with previous results that have implicated many global processes in antibiotic tolerance including heterogeneity in growth state (22, 52, 53) and enhanced expression of drug efflux pumps (54, 55). This is also consistent with the relatively weak correlation in expression between *sasA* and the constitutive promoter *veg* (Fig. S2). Indeed, it remains to be seen precisely how cellular physiology changes in a *sasA*-expression dependent manner. SasA has been shown to be important for ribosome assembly in *B. subtilis* (29) and for survival during envelope stress in *S. aureus* (56). More generally, various cellular processes are known to be directly and indirectly affected by rising (p)ppGpp levels including inhibition of DNA primase activity (57), and reduction in intracellular GTP pools (58) thereby downregulating rRNA transcription (59). As our results show that antibiotic survival increases continuously with *sasA* expression, it suggests that SasA exerts a continuous effect proportional to its level on

296 physiological processes that mediate ciprofloxacin killing. Therefore, multisite phosphorylation
297 may provide a “bet-hedging” strategy to regulate the phenotypic diversity of a bacterial population,
298 serving as a broadly useful mechanism to tune the frequency of rare phenotypes that facilitate
299 survival under adverse conditions.
300

References:

1. Arnoldini M*, et al.* (2014) Bistable expression of virulence genes in salmonella leads to the formation of an antibiotic-tolerant subpopulation. *PLoS Biol* 12(8):e1001928.
2. Norman TM, Lord ND, Paulsson J, & Losick R (2015) Stochastic Switching of Cell Fate in Microbes. *Annual review of microbiology* 69:381-403.
3. Maamar H, Raj A, & Dubnau D (2007) Noise in gene expression determines cell fate in Bacillus subtilis. *Science* 317(5837):526-529.
4. Gunawardena J (2005) Multisite protein phosphorylation makes a good threshold but can be a poor switch. *Proc Natl Acad Sci U S A* 102(41):14617-14622.
5. Ortega F, Garces JL, Mas F, Kholodenko BN, & Cascante M (2006) Bistability from double phosphorylation in signal transduction. Kinetic and structural requirements. *FEBS J* 273(17):3915-3926.
6. Wright DP & Ulijasz AT (2014) Regulation of transcription by eukaryotic-like serine-threonine kinases and phosphatases in Gram-positive bacterial pathogens. *Virulence* 5(8):863-885.
7. Laub MT & Goulian M (2007) Specificity in two-component signal transduction pathways. *Annu Rev Genet* 41:121-145.
8. Batchelor E & Goulian M (2003) Robustness and the cycle of phosphorylation and dephosphorylation in a two-component regulatory system. *Proc Natl Acad Sci U S A* 100(2):691-696.
9. Shinar G, Milo R, Martinez MR, & Alon U (2007) Input output robustness in simple bacterial signaling systems. *Proc Natl Acad Sci U S A* 104(50):19931-19935.
10. Batchelor E, Silhavy TJ, & Goulian M (2004) Continuous control in bacterial regulatory circuits. *J Bacteriol* 186(22):7618-7625.
11. Miyashiro T & Goulian M (2008) High stimulus unmasks positive feedback in an autoregulated bacterial signaling circuit. *Proc Natl Acad Sci U S A* 105(45):17457-17462.
12. Roggiani M & Goulian M (2015) Oxygen-Dependent Cell-to-Cell Variability in the Output of the Escherichia coli Tor Phosphorelay. *J Bacteriol* 197(12):1976-1987.
13. Carey JN*, et al.* (2018) Regulated Stochasticity in a Bacterial Signaling Network Permits Tolerance to a Rapid Environmental Change. *Cell*.
14. Bigger JW (1944) Treatment of staphylococcal infections with penicillin by intermittent sterilisation. *Lancet* 244:497–500.
15. Fauvart M, De Groote VN, & Michiels J (2011) Role of persister cells in chronic infections: clinical relevance and perspectives on anti-persister therapies. *J Med Microbiol* 60(Pt 6):699-709.
16. Abranches J*, et al.* (2009) The molecular alarmone (p)ppGpp mediates stress responses, vancomycin tolerance, and virulence in Enterococcus faecalis. *J Bacteriol* 191(7):2248-2256.
17. Gaca AO*, et al.* (2013) Basal levels of (p)ppGpp in Enterococcus faecalis: the magic beyond the stringent response. *MBio* 4(5):e00646-00613.

18. Dordel J*, et al.* (2014) Novel determinants of antibiotic resistance: identification of mutated loci in highly methicillin-resistant subpopulations of methicillin-resistant Staphylococcus aureus. *MBio* 5(2):e01000.

19. Maisonneuve E & Gerdes K (2014) Molecular mechanisms underlying bacterial persisters. *Cell* 157(3):539-548.

20. Liu K, Bittner AN, & Wang JD (2015) Diversity in (p)ppGpp metabolism and effectors. *Curr Opin Microbiol* 24:72-79.

21. Nguyen D*, et al.* (2011) Active starvation responses mediate antibiotic tolerance in biofilms and nutrient-limited bacteria. *Science* 334(6058):982-986.

22. Balaban NQ, Merrin J, Chait R, Kowalik L, & Leibler S (2004) Bacterial persistence as a phenotypic switch. *Science* 305(5690):1622-1625.

23. Maisonneuve E, Castro-Camargo M, & Gerdes K (2013) (p)ppGpp Controls Bacterial Persistence by Stochastic Induction of Toxin-Antitoxin Activity. *Cell* 154(5):1140-1150.

24. Cashel M, Gentry D, Hernandez V, & Vinella D (1996) The stringent response in Escherichia coli and Salmonella typhimurium. *Escherichia coli and Salmonella; Cellular and Molecular Biology*, (ASM Press, Washington DC), Vol 2, pp 1458-1496.

25. Atkinson GC, Tenson T, & Hauryliuk V (2011) The RelA/SpoT homolog (RSH) superfamily: distribution and functional evolution of ppGpp synthetases and hydrolases across the tree of life. *PLoS One* 6(8):e23479.

26. Nanamiya H*, et al.* (2008) Identification and functional analysis of novel (p)ppGpp synthetase genes in Bacillus subtilis. *Mol Microbiol* 67(2):291-304.

27. D'Elia MA*, et al.* (2009) Probing teichoic acid genetics with bioactive molecules reveals new interactions among diverse processes in bacterial cell wall biogenesis. *Chem Biol* 16(5):548-556.

28. Eiamphungporn W & Helmann JD (2008) The Bacillus subtilis sigma(M) regulon and its contribution to cell envelope stress responses. *Mol Microbiol* 67(4):830-848.

29. Tagami K*, et al.* (2012) Expression of a small (p)ppGpp synthetase, YwaC, in the (p)ppGpp(0) mutant of Bacillus subtilis triggers YvyD-dependent dimerization of ribosome. *MicrobiologyOpen* 1(2):115-134.

30. Gaidenko TA, Kim TJ, & Price CW (2002) The PrpC serine-threonine phosphatase and PrkC kinase have opposing physiological roles in stationary-phase Bacillus subtilis cells. *J Bacteriol* 184(22):6109-6114.

31. Libby EA, Goss LA, & Dworkin J (2015) The Eukaryotic-Like Ser/Thr Kinase PrkC Regulates the Essential WalRK Two-Component System in Bacillus subtilis. *PLoS Genet* 11(6):e1005275.

32. Elowitz MB, Levine AJ, Siggia ED, & Swain PS (2002) Stochastic gene expression in a single cell. *Science* 297(5584):1183-1186.

33. Leveau JH & Lindow SE (2001) Predictive and interpretive simulation of green fluorescent protein expression in reporter bacteria. *J Bacteriol* 183(23):6752-6762.

34. Radeck J*, et al.* (2013) The Bacillus BioBrick Box: generation and evaluation of essential genetic building blocks for standardized work with Bacillus subtilis. *J Biol Eng* 7(1):29.

35. Thackray PD & Moir A (2003) SigM, an extracytoplasmic function sigma factor of Bacillus subtilis, is activated in response to cell wall antibiotics, ethanol, heat, acid, and superoxide stress. *J Bacteriol* 185(12):3491-3498.

36. Salzberg LI*, et al.* (2013) The WalRK (YycFG) and sigma(I) RsgI regulators cooperate to control CwlO and LytE expression in exponentially growing and stressed Bacillus subtilis cells. *Mol Microbiol* 87(1):180-195.

37. Dubrac S, Bisicchia P, Devine KM, & Msadek T (2008) A matter of life and death: cell wall homeostasis and the WalKR (YycGF) essential signal transduction pathway. *Mol Microbiol* 70(6):1307-1322.

38. Jones DL, Brewster RC, & Phillips R (2014) Promoter architecture dictates cell-to-cell variability in gene expression. *Science* 346(6216):1533-1536.

39. Sanchez A, Garcia HG, Jones D, Phillips R, & Kondev J (2011) Effect of promoter architecture on the cell-to-cell variability in gene expression. *PLoS Comput Biol* 7(3):e1001100.

40. Shah IM, Laaberki MH, Popham DL, & Dworkin J (2008) A eukaryotic-like Ser/Thr kinase signals bacteria to exit dormancy in response to peptidoglycan fragments. *Cell* 135(3):486-496.

41. Kriel A*, et al.* (2014) GTP dysregulation in Bacillus subtilis cells lacking (p)ppGpp results in phenotypic amino acid auxotrophy and failure to adapt to nutrient downshift and regulate biosynthesis genes. *J Bacteriol* 196(1):189-201.

42. Fisher RA, Gollan B, & Helaine S (2017) Persistent bacterial infections and persister cells. *Nat Rev Microbiol* 15(8):453-464.

43. Hahn J, Tanner AW, Carabetta VJ, Cristea IM, & Dubnau D (2015) ComGA-RelA interaction and persistence in the Bacillus subtilis K-state. *Mol Microbiol* 97(3):454-471.

44. Germain E, Castro-Roa D, Zenkin N, & Gerdes K (2013) Molecular mechanism of bacterial persistence by HipA. *Mol Cell* 52(2):248-254.

45. Levin-Reisman I*, et al.* (2017) Antibiotic tolerance facilitates the evolution of resistance. *Science* 355(6327):826-830.

46. Ferrell JE, Jr. & Ha SH (2014) Ultrasensitivity part II: multisite phosphorylation, stoichiometric inhibitors, and positive feedback. *Trends Biochem Sci* 39(11):556-569.

47. Nash P*, et al.* (2001) Multisite phosphorylation of a CDK inhibitor sets a threshold for the onset of DNA replication. *Nature* 414(6863):514-521.

48. Zaytsev AV*, et al.* (2015) Multisite phosphorylation of the NDC80 complex gradually tunes its microtubule-binding affinity. *Mol Biol Cell* 26(10):1829-1844.

49. Pufall MA*, et al.* (2005) Variable control of Ets-1 DNA binding by multiple phosphates in an unstructured region. *Science* 309(5731):142-145.

50. Shaffer SM*, et al.* (2017) Rare cell variability and drug-induced reprogramming as a mode of cancer drug resistance. *Nature* 546(7658):431-435.

51. Kester JC & Fortune SM (2014) Persisters and beyond: mechanisms of phenotypic drug resistance and drug tolerance in bacteria. *Crit Rev Biochem Mol Biol* 49(2):91-101.

52. Conlon BP*, et al.* (2016) Persister formation in Staphylococcus aureus is associated with ATP depletion. *Nature microbiology* 1:16051.

53. Gutierrez A*, et al.* (2017) Understanding and Sensitizing Density-Dependent Persistence to Quinolone Antibiotics. *Mol Cell* 68(6):1147-1154 e1143.

54. Adams KN*, et al.* (2011) Drug tolerance in replicating mycobacteria mediated by a macrophage-induced efflux mechanism. *Cell* 145(1):39-53.

55. Pu Y*, et al.* (2016) Enhanced Efflux Activity Facilitates Drug Tolerance in Dormant Bacterial Cells. *Mol Cell* 62(2):284-294.

56. Geiger T, Kastle B, Gratani FL, Goerke C, & Wolz C (2014) Two small (p)ppGpp synthases in Staphylococcus aureus mediate tolerance against cell envelope stress conditions. *J Bacteriol* 196(4):894-902.

57. Wang JD, Sanders GM, & Grossman AD (2007) Nutritional control of elongation of DNA replication by (p)ppGpp. *Cell* 128(5):865-875.

58. Kriel A*, et al.* (2012) Direct regulation of GTP homeostasis by (p)ppGpp: a critical component of viability and stress resistance. *Mol Cell* 48(2):231-241.

59. Krasny L & Gourse RL (2004) An alternative strategy for bacterial ribosome synthesis: Bacillus subtilis rRNA transcription regulation. *EMBO J* 23(22):4473-4483.

Acknowledgements:

We thank Eric Brown for the strain EB1385, Isaac Plant (Silver lab) for the plasmid pIP384, and Amir Figueroa at the Microbiology & Immunology Core Facility at Columbia University for assistance with flow cytometry and cell sorting. This work was supported by NIH GM114213 and a BWF Investigators in the Pathogenesis of Infectious Disease award to JD, a grant from the Department of Systems Biology at Harvard Medical School to EAL, and SR was supported by NIH GM095784 and gratefully acknowledges support from the Azrieli Foundation. Author Contributions: Conceived and designed the experiments EAL and JD. EAL performed the experiments. EAL and SR analyzed data. Contributed reagents/materials/analysis tools: EAL and SR. Wrote the paper: EAL, SR and JD.

Figures and Figure Legends

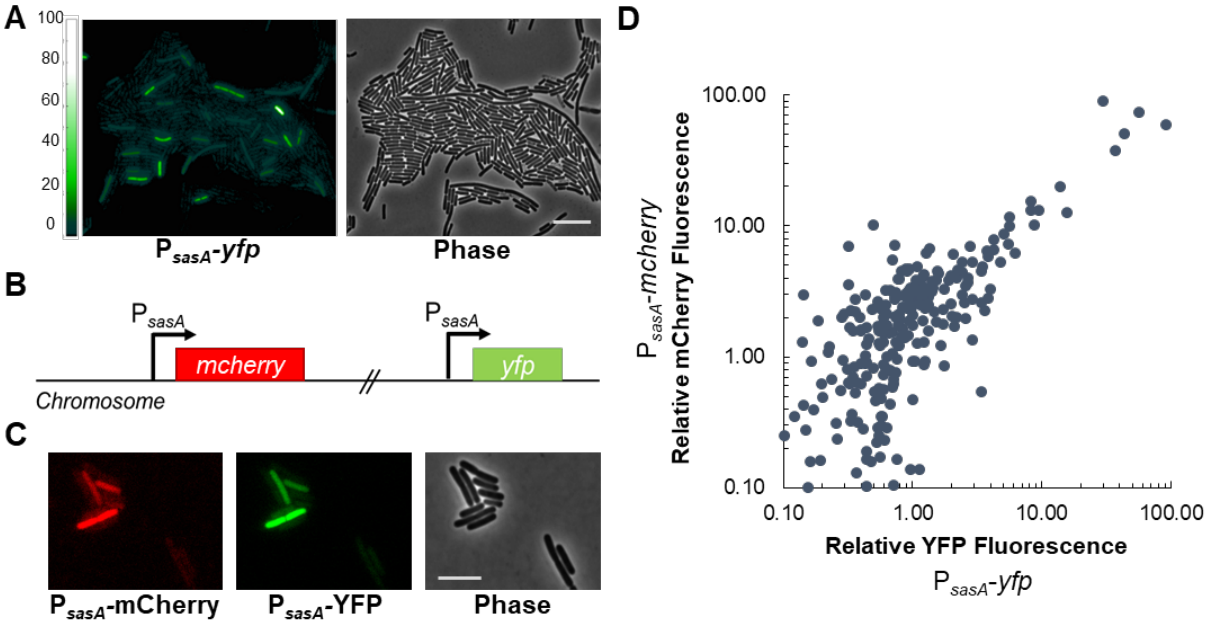

Figure 1: *sasA* exhibits cell-to-cell variability in expression.

A) P_{sasA}-*yfp* expression in log phase culture. **Left:** YFP image. Color scale indicates the fold change relative to the population average. **Right:** Phase contrast. Scale bar indicates 10 μm.

B) Schematic of dual-color transcriptional reporter strain to characterize the noise in *sasA* expression. Two copies of the *sasA* promoter driving different reporters (P_{sasA}-*yfp*, P_{sasA}-*mcherry*) are inserted at separate ectopic loci.

C) Evidence for extrinsic noise in *sasA* expression**.** Images of single cells from the dual reporter strain with significant fluorescence shown in mCherry (**Left**), YFP (**Center**), and phase contrast (**Right**) channels. Scale bar indicates 5 μm.

D) Quantification of cellular fluorescence intensities for single cells in the experiment described in **B,C**. Values were normalized relative to the population mean value for each channel. Data shown was measured on ~ 580 cells with detectable fluorescence in both channels. The fluorescence of the two reporters have a Pearson's correlation coefficient of r ~ 0.90±0.08 (SEM). For each reporter, the CV ~ 4.95±0.42 (SEM).

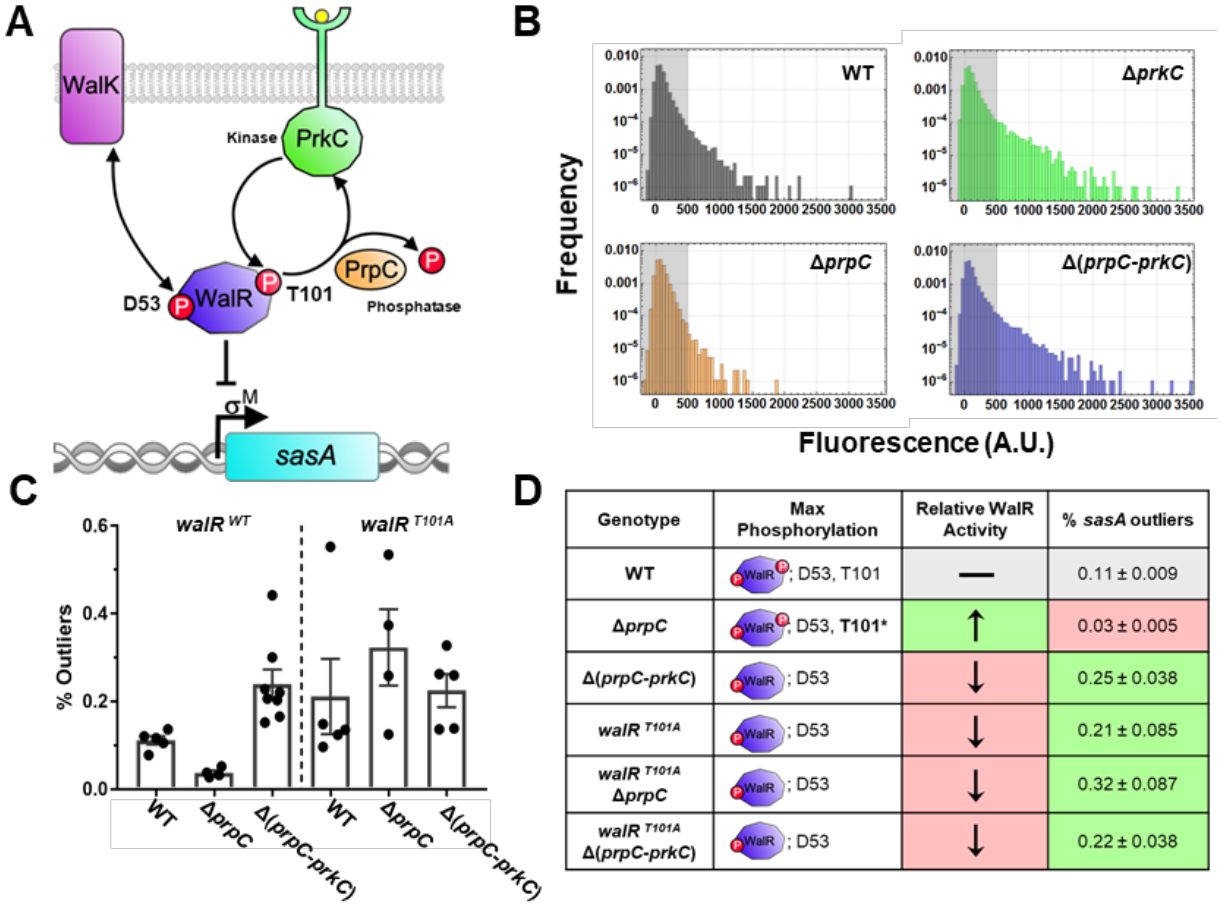

Genotype	Max Phosphorylation	Relative WalR Activity	% *sasA* outliers
WT	WalR~P; D53, T101	—	0.11 ± 0.009
Δ*prpC*	WalR~P; D53, **T101***	↑	0.03 ± 0.005
Δ(*prpC-prkC*)	WalR~P; D53	↓	0.25 ± 0.038
walR T101A	WalR~P; D53	↓	0.21 ± 0.085
walR T101A Δ*prpC*	WalR~P; D53	↓	0.32 ± 0.087
walR T101A Δ(*prpC-prkC*)	WalR~P; D53	↓	0.22 ± 0.038

Figure 2: The Ser/Thr kinase PrkC and phosphatase PrpC regulate cell-to-cell variability in *sasA*

A) Model for PrkC-dependent regulation of *sasA*. WalR binding to the *sasA* promoter represses *sasA*. WalR activity is primarily controlled by phosphorylation on Asp 53 by its cognate histidine kinase WalK, and secondarily by phosphorylation on Thr 101 by the Ser/Thr kinase PrkC. WalR T101~P can be dephosphorylated by the phosphatase PrpC. T101~P further enhances the repressing activity of WalR D53~P, resulting in lower expression of *sasA* under conditions with high Thr 101~P (e.g., Δ*prpC*). Under conditions lacking Thr 101~P (*e.g.,* Δ*prkC*), the increased repression of *sasA* is relieved.

B) Histograms demonstrating PrkC-dependent cell-to-cell variability in *sasA*. P_{sasA}-*yfp* reporter activity was quantified by flow cytometry in wild type (WT, gray), Δ*prpC* (orange), Δ*prkC* (green), and Δ(*prpC-prkC*) (blue) backgrounds. Shaded region of each plot indicates the range of cellular autofluorescence observed. Each histogram was computed from data on ~$3.0*10^4$ events.

C) Percentage of outliers in each genetic background. At least 4 independent experiments, similar to and including the representative one shown in **B**, were performed in *walR* ^{WT} (**Left**) and *walR* ^{T101A} (**Right**) backgrounds. Each experiment was normalized to a control and outliers were defined as cells above a fixed threshold level of normalized fluorescence (~1250 A.U.). Dots represent the percentage of each population that is above the threshold; bars and lines represent the mean and SEM, respectively.

D) Summary of each genotype, its effect on the maximal occupancy of the two known WalR phosphosites, and the expected effect on WalR activity relative to WT. For each genotype the mean percentage of outliers in *sasA* expression (shown in **C**) are also summarized. Note that in the Δ*prpC* background, the T101 phosphorylation is stabilized (denoted as **T101***).

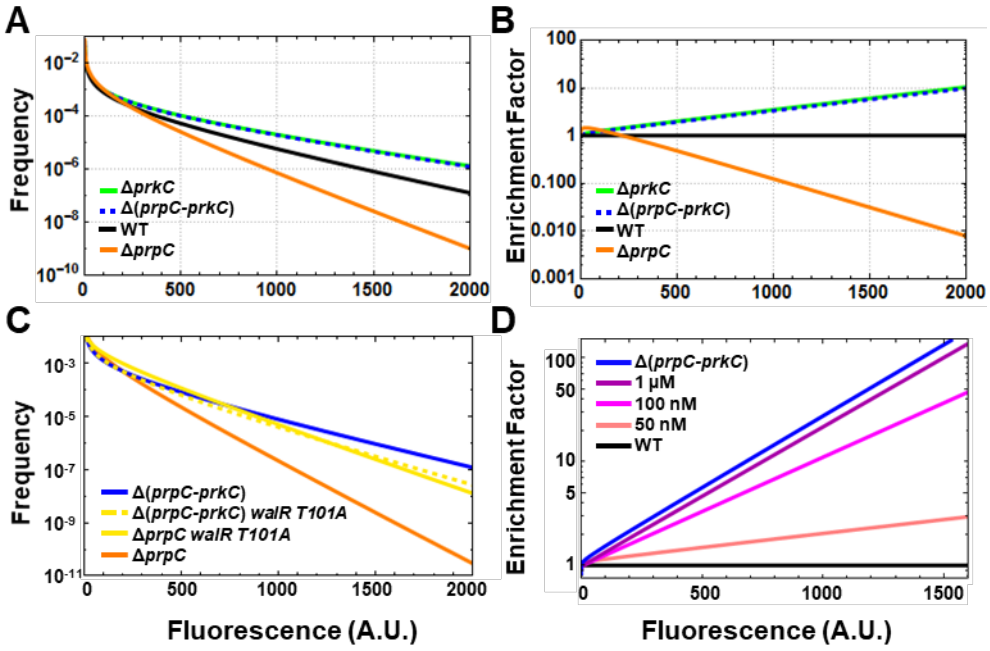

Figure 3: Multisite phosphorylation causes exponential changes in abundance of cells with a given level of *sasA* expression

A) Functional fits of autofluorescence-free distributions of *sasA* expression. A deconvolution algorithm was used to remove the contribution of autofluorescence from the measured distributions of *sasA* expression shown in Figure 2B. Validation of the fits are shown in Fig. S5.

B) Effect of PrkC on the distribution of *sasA* expression. For each genotype in **A** the frequency of cells with a given level of *sasA* expression was normalized against the equivalent frequency in the WT population. On this semi-logarithmic plot, straight lines indicate that the enrichment factor changes ~exponentially with fluorescence.

C) PrkC-dependent regulation of cell-to-cell variability in *sasA* is WalR Thr-101-dependent. P_{sasA}-*yfp* reporter activity was quantified by flow cytometry in a Δ*prpC walR T101A* (yellow, solid) background and compared to Δ*prpC* (orange), Δ(*prpC-prkC*) (blue), and Δ(*prpC-prkC*) *walR T101A* (yellow, dashed) backgrounds in the

same experiment. Plots were generated by applying the deconvolution method described in **A** to the measured data in Fig. S6A.

D) Gradual inhibition of PrkC results in progressive enrichment of cells with elevated levels of *sasA*. P_{sasA}-*yfp* reporter activity was quantified by flow cytometry during treatment with increasing concentrations of staurosporine: 0 (solvent only; black), 50, 100 nM, and 1 µM (shades of magenta), in otherwise WT populations. For reference, a Δ(*prpC-prkC*) (blue) population treated with solvent only is shown; note that the effect of staurosporine saturates at this level. Plots were generated by applying the deconvolution method described in **A** to the measured data in Fig. S6B,C. For each condition the frequency of cells with a given level of *sasA* expression was normalized against the equivalent frequency in the WT population. As in **B**, straight lines indicate that enrichment grows ~exponentially with fluorescence. Enrichment becomes more pronounced as the concentration of staurosporine increases and saturates at the level of complete inhibition ~Δ(*prpC-prkC*).

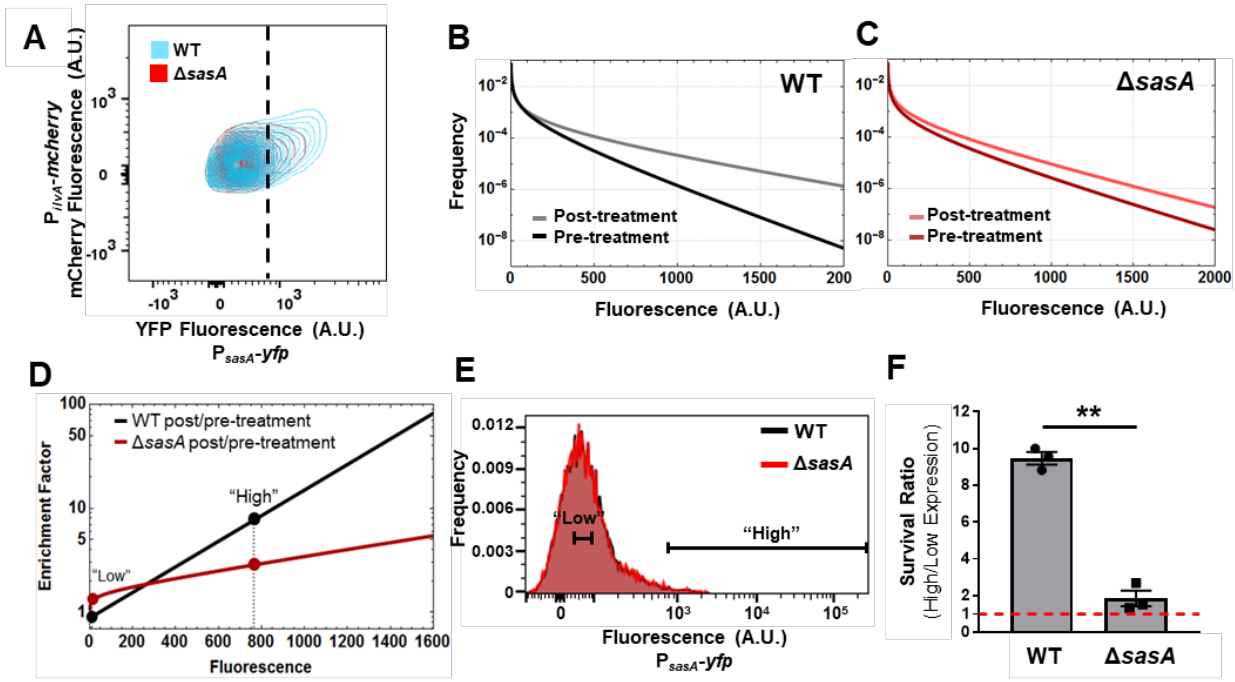

Figure 4: Cells with elevated *sasA* expression preferentially survive antibiotic treatment

A) The distribution of *ilvA* (mCherry) and *sasA* expression (YFP) in single cells. Shown are contour plots of wild type (WT; blue) and Δ*sasA* (red) populations treated with 100 µg/ml bacitracin to induce *sasA* expression. Contour lines shown are at 2% levels. A correlated increase in *ilvA* expression is observed in WT cells with *sasA* levels greater than the dashed line. Data represents ~3.0*10^4 events for each population.

B) Autofluorescence-free distributions of *sasA* expression before (dark gray) and after (light gray) ciprofloxacin treatment in an otherwise WT background based on the data shown in Fig. S8A.

C) Autofluorescence-free distributions of *sasA* expression before (dark red) and after (light red) ciprofloxacin treatment in a Δ*sasA* background based on the data shown in Fig. S8B.

D) Enrichment plot following antibiotic treatment for WT and Δ*sasA* populations. For each genotype in **B** and **D** the frequency of cells with a given level of P_{sasA}-*yfp* after antibiotic

542 treatment was normalized against the corresponding frequency prior to antibiotic
543 treatment. Dashed lines indicate the average values used in **E** and **F**.

544 **E)** Histograms of P_{sasA}-*yfp* fluorescence in WT (black) and Δ*sasA* (red) backgrounds
545 measured by flow cytometry prior to sorting into "low" (4.1 ± 1.8) or "high" (779.5 ±
546 134.9) expression groups (relative mean ± SEM, 3 experiments). Each histogram is
547 comprised of data obtained from ~$3.0*10^4$ events and is from a representative
548 experiment used in **F**.

549 **F)** Relative survival of the "high" and "low" expression populations in **E** after treatment with
550 ciprofloxacin for ~3.5 h as in **B,C**. Bars indicate the mean survival ratio of the "high" to
551 "low" expressing populations. The data shown represents 3 independent experiments
552 (paired t-test, p-value ~ 0.009, **). The red dashed line represents a survival ratio of 1,
553 indicating no advantage.